

Investigation on Effects of Addition of Cations [Li^+ , Na^+ , K^+ , Ag^+] on Luminescence Intensity of $\text{LaAlO}_3:\text{Eu}^{3+}$ Nano-Phosphors Prepared by Combustion Synthesis

Subhash Chand¹, Ishwar Singh²

¹Department of Chemistry, Maharshi Dayanand University, Rohtak-124001, Haryana, India

² PDM University, Sector 3A, Sarai Aurangabad, Bahadurgarh-124507, Haryana, India

Abstract: $\text{LaAlO}_3:\text{Eu}^{3+}$, [Li^+ , Na^+ , K^+ , Ag^+] nano-phosphors with varying dopant concentrations of Eu^{3+} from 3 to 18 mol% & codopants concentration of [Li^+ , Na^+ , K^+ , Ag^+] from 1 to 2mol% were prepared by combustion synthesis method and the samples were further heated to 1,000 °C to improve the crystallinity of the materials. The structure and morphology of materials have been examined by X-ray diffraction and scanning electron microscopy. SEM images depicted that the morphology of crystallites have uniform shapes and sizes. Small and coagulated particles of regular shapes of different sizes are obtained. The characteristic emissions of Eu^{3+} were clearly observed at nearly 580, 590, 618, 649 to 709 (multiplet structure) nm for $^5\text{D}_0 \rightarrow ^7\text{F}_n$ transitions where $n = 0, 1, 3, 4$ respectively, including the strongest red emission peaks at 618 nm for $^5\text{D}_0 \rightarrow ^7\text{F}_2$ transitions in $\text{LaAlO}_3:\text{Eu}^{3+}$ host lattices but intensity of emission peak corresponding to $^5\text{D}_0 \rightarrow ^7\text{F}_1$ transitions in $\text{LaAlO}_3:\text{Eu}^{3+}$ material is less as compared to that of $^5\text{D}_0 \rightarrow ^7\text{F}_2$ transitions which is also a singlet. Other transitions have very weak peaks. Highest photoluminescence intensity is observed with 5 mol% doping of Eu^{3+} with 1 mol % of K^+ made LaAlO_3 makes it a strong competitor for red colored display applications.

Keywords: Combustion synthesis, Nano-phosphors, $\text{LaAlO}_3:\text{Eu}^{3+}$, Host lattices, Codopants

1. Introduction

Rare-earth ions (Tb^{3+} , Pr^{3+} , Eu^{3+} , Sm^{3+} , La^{3+} etc.) have been widely used as luminescent centers in phosphor materials due to their sharp 4f-intra shell transitions [1-3]. Among these ions, europium is most widely used activator and has been used in phosphor materials for an efficient red and blue emission. The europium emission in the phosphor material is strongly dependent on the host lattice and it is possible to obtain different colors from blue to red. Europium can act as an activator in two forms, viz. Eu^{2+} and Eu^{3+} . These two states can be identified from their characteristic photoluminescence spectrum [4]. Recently, optical properties of the trivalent europium (Eu^{3+}) doped crystals and glasses have been studied by several research groups. They have investigated Eu^{3+} emission in borates, oxides, silicates, phosphates, sulfates and fluorides [5-10], etc. These materials find their applications in lighting, information display, and optoelectronics technology. The photoluminescence properties of RE-doped compounds not only depend on the composition and local structure of the host but also affected by its crystal size and morphology. It is our main interest to synthesize yet another family of newly developed Eu^{3+} doped phosphors via low temperature initiated combustion process and investigate their photoluminescence properties in view of the commercial importance of reddish-orange color emitting phosphors. The emission and absorption spectra of $\text{LaAlO}_3:\text{Eu}^{3+}$ nano crystals have been investigated and detailed mechanism of luminescence has been proposed in literature by many investigators [11, 12]. The mixed emission consisting of Eu^{2+} and Eu^{3+} in LaAlO_3 has been reported by Mao et. al.[4]. There are very few references about the luminescence

properties of $\text{CsAlO}_2:\text{Eu}^{3+}$ and $\text{LiLaO}_2:\text{Eu}^{3+}$ phosphors though their crystal structures are identified in literature [13, 14]. The structure of CsAlO_2 has been interpreted in the light of Zintl-Klemm concept [13] as if the alkali metal atoms would donate electrons to the Al atoms. The stoichiometric compounds like MAIO_2 crystallized as stuffed cristobalites in which the Al array adopts the diamond like structure of Si[13]. The LiLaO_2 material is found to have α - NaFeO_2 -related crystal structure [14], but Abbattista and Vallino [15] concluded from the study of the La_2O_3 - Li_2O binary system between 750°C and 1000°C where LaLiO_2 occurs as the only binary compound. It is characterized by a monoclinic cell ($a = 5.88 \text{ \AA}$; $b = 6.22 \text{ \AA}$; $c = 584 \text{ \AA}$; $\beta = 102.53^\circ$) and is isomorphous with α - EuLiO_2 . Any orthorhombic polymorph of this compound is excluded between 750°C to 1000°C. As we know different material preparation methods have some important effects on material microstructure and physical properties. The combustion method provides an interesting alternative over other elaborated techniques because it offers several attractive advantages such as: simplicity of experimental set-up; surprisingly short time between the preparation of reactants and the availability of the final product; and being cheap due to energy saving. The main aim of the combustion method is the rapid decomposition of the rare earth nitrate in the presence of an organic fuel. During the reaction, many gases, such as CO_2 , N_2 , NO_2 and H_2O , as well as a large amount of heat are released in a short period of time before the process terminates with white, foamy and crispy products. Many times final products are found to be composed of nanosized particles. This work has been carried out with the aim to prepare, compare and investigate the high intensity photoluminescence nanosized crystalline powders of LaAlO_3 doped with Eu^{3+} and co-

Volume 6 Issue 2, February 2017

www.ijsr.net

Licensed Under Creative Commons Attribution CC BY

doped with some monovalent metal ions [Li^+ , Na^+ , K^+ , Ag^+] sintered at 1000°C temperature. The crystalline structure and morphology of prepared nano-materials have also been discussed. The crystalline structure of prepared materials, morphology of particles and their photoluminescence properties are characterized by XRD, SEM and PL spectra with 325 nm lasers for excitation.

2. Experimental

Synthesis of $\text{La}_{(1-x)}\text{AlO}_3 : \text{Eu}^{3+} \text{M}^+$ phosphor by Combustion Method

High purity chemicals $\text{La}(\text{NO}_3)_3$, $\text{Al}(\text{NO}_3)_3$ [1.0mole], $\text{Eu}(\text{NO}_3)_3$, LiNO_3 , NaNO_3 , KNO_3 , AgNO_3 in such a way that total $\text{La}^{3+} + [\text{Eu}^{3+} + \text{M}^+] = 1.0$ mole, and hexamethylenetetramine as a fuel were used to prepare Eu^{3+} doped nano crystals with general formula $\text{La}_{(1-x)}\text{AlO}_3 : \text{Eu}_x^{3+}$ & where x is 3 to 18 mol%, $\text{La}_{(1-x+y)}\text{AlO}_3 : \text{Eu}_x^{3+} \cdot \text{M}_y^+$ where y is 1 to 2 mol%, by heating rapidly an aqueous concentrated paste in a preheated furnace maintained at 550°C . The stoichiometric amount of the fuel was calculated by using total oxidizing and reducing valences [16]. The paste was made by dissolving metal nitrates and fuel in a minimum amount of doubly distilled water. In furnace, the material had rapid dehydration followed by decomposition, generating combustible gases which burnt with a flame and producing a white solid. The solid thus obtained was again fired at 1000°C for 3h to increase the crystallinity. Finally the powder was characterized by XRD, SEM, PL measurement to check the crystallinity, particles size and luminescence intensity of the phosphor respectively.

3. Characterization & Discussion

3.1 XRD Studies

The structural characterizations of compounds were done on XRD diffractometer (Rigaku Ultima IV) using $\text{Cu K}\alpha$ radiation (1.541841 \AA). The structural characterizations of compounds were done on XRD diffractometer (Rigaku Ultima IV) using $\text{Cu K}\alpha$ radiation. Figures 1 showed the X-ray diffractograms of Eu^{3+} doped LaAlO_3 powders. The phase analysis demonstrated (Fig.1) that $\text{LaAlO}_3 : \text{Eu}^{3+}$ belongs to trigonal crystal system with $R\bar{3}m$ (160) space group having unit cell dimensions: $a = b = 5.364 \text{ \AA}$ and $c = 13.11 \text{ \AA}$. This was in good agreement with the standard JCPDS C. NO. 031-0022.

In this phosphor, trivalent lanthanum ions were replaced by trivalent europium ions. Dopant ions (Eu^{3+}) concentration variation from 3mol % to 20 mol% have no noticeable effect on the obtained X-ray diffractograms of the as-prepared $\text{LaAlO}_3 : \text{Eu}^{3+}$ phosphors, indicating that the doped ions were occupied the primordial La^{3+} sites of the LaAlO_3 lattice. All measurements were carried out at room temperature.

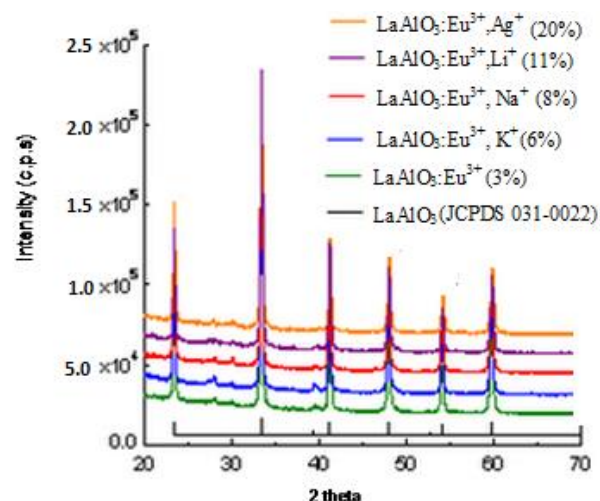


Figure 1: XRD spectra of $\text{LaAlO}_3 : \text{Eu}^{3+} [\text{Li}^+, \text{Na}^+, \text{K}^+, \text{Ag}^+]$ phosphors

The structural characterization was done by a high resolution X-ray diffraction (XRD) using a Rigaku Ultima IV diffractometer in the θ - 2θ configuration and using $\text{Cu K}\alpha$ radiation (1.5418 \AA) using Scherrer equation (1).

$$\tau = K\lambda / \beta \cos \theta \quad (1)$$

where

- τ is the mean size of the ordered (crystalline) domains, which may be smaller or equal to the grain size;
- K is a dimensionless shape factor, with a value close to unity. The shape factor has a typical value of about 0.9, but varies with the actual shape of the crystallite;
- λ is the X-ray wavelength;
- β is the line broadening at half the maximum intensity (FWHM), after subtracting the instrumental line broadening, in radians. This quantity is sometimes denoted as (2θ) ;
- θ is the Bragg angle was used to calculate the crystallite size of all materials.

At least five prominent peaks from each XRD (samples with various Eu^{3+} concentration) were used for calculation and peaks belonging to different phases were also taken into consideration. Maximum and minimum values obtained for each type of lattice are reported as range of crystallite size (e.g. $30\text{--}40 \pm 5 \text{ nm}$ for LaAlO_3).

3.2 SEM micrograph and particle size analysis

The SEM micrographs were obtained by JEOL JSM6300 scanning electron microscope. Figures 2 (a to f) exhibited the surface morphologies of LaAlO_3 , $\text{LaAlO}_3 : \text{Eu}^{3+}$ and $\text{LaAlO}_3 : \text{Eu}^{3+}, [\text{Li}^+, \text{Na}^+, \text{K}^+, \text{Ag}^+]$ particles. It is clear from SEM images that the morphology of crystallites have no uniform shapes and particles size lie within average range of $40 \pm 5 \text{ nm}$. Generally non-uniformity of shape and size is associated with the non-uniform distribution of temperature and mass flow in the combustion flame. Several pores are observed in SEM images (fig. 2 a, b) which are formed by the escaping gases during the combustion reaction. Also, several small particles can be seen within grains.

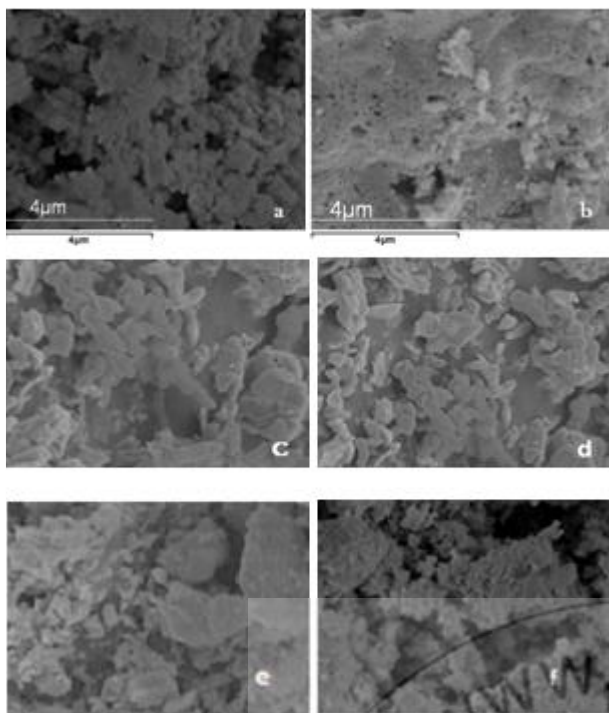


Figure 2: SEM micrographs of phosphor particles (a,b,c,d,e,f): (a) LaAlO_3 lattice (b) $\text{LaAlO}_3:\text{Eu}^{3+}$ (c) $\text{LaAlO}_3:\text{Eu}^{3+}, [\text{Li}^+]$ (d) $\text{LaAlO}_3:\text{Eu}^{3+}, [\text{Na}^+]$ (e) $\text{LaAlO}_3:\text{Eu}^{3+}, [\text{K}^+]$ & (f) $\text{LaAlO}_3:\text{Eu}^{3+}, [\text{Ag}^+]$

Above mentioned features are inherent in combustion derived powders. However the SEM images of $\text{LaAlO}_2:\text{Eu}^{3+}$ particles (fig. 2a,b) show small and coagulated particles of nearly cubical shape with larger size distribution. The surface morphology of $\text{LaAlO}_2:\text{Eu}^{3+}$ lattices as depicted in the picture 2a and 2b is smooth and coagulated particles of irregular elliptical shapes with different sizes are observed. The smooth surface of phosphor can reduce the non-radiation and scattering, thus beneficial to the luminescence efficiency in application[19]. The dense packed small particles can prevent the phosphor from aging.

3.2 Photoluminescence Properties

For the photoluminescence measurement, 0.05g powder samples were pressed into pellets and then exposed to a He-Cd laser (325nm) with an optical power of 30mW for excitation. The emitted light was analyzed by HR-4000 Ocean Optics USB spectrometer optimized for the UV-vis range. The room-temperature emission spectra of Eu^{3+} doped LaAlO_3 crystals with different doping concentrations are shown in figures 3 (a to b). The emission spectra were obtained by monitoring at 325nm under an excitation of ultraviolet light. The obtained products emitted the red luminescence of varying intensities, which showed the activator Eu^{3+} had successfully entered the host lattice of LaAlO_3 . The characteristic emissions of Eu^{3+} were clearly observed with sharp and strong peaks at 612-625 nm for $^5\text{D}_0 \rightarrow ^7\text{F}_2$ transition, and others at nearly 536-576 nm, 580-596 nm, 648-652 nm, 681-709 nm for $^5\text{D}_0 \rightarrow ^7\text{F}_n$ transitions where n= 0,1,3,4 respectively. The exact positions of emission peaks in various lattices are shown in table 1.

Table 1: The emission peaks in $\text{LaAlO}_3:\text{Eu}^{3+}, [\text{Li}^+, \text{Na}^+, \text{K}^+, \text{Ag}^+]$ nano-phosphors

Lattice	$^5\text{D}_0 \rightarrow ^7\text{F}_0$ (nm)	$^5\text{D}_0 \rightarrow ^7\text{F}_1$ Orange-red (nm)	$^5\text{D}_0 \rightarrow ^7\text{F}_2$ Red (nm)	$^5\text{D}_0 \rightarrow ^7\text{F}_3$ (nm)	$^5\text{D}_0 \rightarrow ^7\text{F}_4$ (nm)
$\text{La}_{0.97}\text{Eu}_{0.03}\text{AlO}_3$	556	591	609	690	707
$\text{La}_{0.94}\text{Eu}_{0.05}\text{K}_{0.01}\text{AlO}_3$	536, 556	582, 591	618	649, 683, 691	700, 704, 709
$\text{La}_{0.92}\text{Eu}_{0.07}\text{Na}_{0.01}\text{AlO}_3$	556	592	617	691	705
$\text{La}_{0.89}\text{Eu}_{0.10}\text{Li}_{0.01}\text{AlO}_3$	555	591	617	690	707
$\text{La}_{0.80}\text{Eu}_{0.18}\text{Ag}_{0.02}\text{AlO}_3$	-----	590	618	691	704

The $^5\text{D}_0 \rightarrow ^7\text{F}_1$ transition is well known to be mainly a magnetic dipole transition when the Eu^{3+} ions locate in a high symmetric position while the $^5\text{D}_0 \rightarrow ^7\text{F}_{2,4}$ transitions are essentially electric dipole transitions which appear dominantly only when Eu^{3+} ion locates at sites without inversion symmetry [17,18]. In fig 3, the emission intensity of all peaks increased with increase of doping concentration from 3% to 5 mol % and then starts decreasing. It becomes nearly one fifth with 20 mol% doping of Eu^{3+} in $\text{LaAlO}_3:\text{Eu}^{3+}$ phosphors. It is expected that with the increase of Eu^{3+} ions, photoluminescence should increase. However, the emission intensity tends to decrease above 5 mol% of Eu^{3+} ions due to concentration quenching, because of non-radiative interaction between ions as the resonant energy transfer becomes stronger. As the concentration is increased, the Eu^{3+} ions are packed closer and closer together, which favors the transfer of energy from one europium ion to the next by a resonance process; the energy eventually reaches a sink from which it is dissipated by non-radiative processes rather than by the emission of visible light [20, 21].

In the present case, the emission spectrum shows two strong sharp peaks at the 591nm and 618nm corresponding to the magnetic dipole transition ($^5\text{D}_0 \rightarrow ^7\text{F}_1$) and electric dipole transition ($^5\text{D}_0 \rightarrow ^7\text{F}_2$) of Eu^{3+} emission respectively. Other weak intensity peaks are seen on either side of strong peaks. Earlier workers also observed these peaks in the Eu^{3+} doped LaAlO_3 host which substantiate the presence of Eu^{3+} ions [10, 11]. The intensity ratio of 591 nm peak to 618 nm peak is a measure of asymmetry of the Eu^{3+} site in the host lattice [22]. Luminescence study shows that magnetic dipole transition ($^5\text{D}_0 \rightarrow ^7\text{F}_1$) is prominent over the electric dipole transition ($^5\text{D}_0 \rightarrow ^7\text{F}_2$), which is attributed to occupancy of inversion symmetry site by more Eu^{3+} ions in Eu^{3+} doped LaAlO_3 . If more Eu^{3+} ions have occupancy at the inversion site, the emission intensity from the $^5\text{D}_0 \rightarrow ^7\text{F}_1$ transition will enhance and the phosphor will primarily exhibit orange luminescence. In the present investigation, the intensity of $^5\text{D}_0 \rightarrow ^7\text{F}_1$ is comparable to $^5\text{D}_0 \rightarrow ^7\text{F}_2$ transition. It may be mentioned that similar results from magnetic dipole transition ($^5\text{D}_0 \rightarrow ^7\text{F}_1$) were observed for Eu^{3+} doped LaAlO_3 host [10-12] and the orange-red emission of the prepared $\text{LaAlO}_3:\text{Eu}^{3+}$ phosphor had already been proposed for its probable utility for display applications. Effect of co-doping of $\text{Li}^+, \text{Na}^+, \text{K}^+$ & Ag^+ ions on $\text{LaAlO}_3:\text{Eu}^{3+}$ structure had been investigated to study the photoluminescent behavior of this lattice.

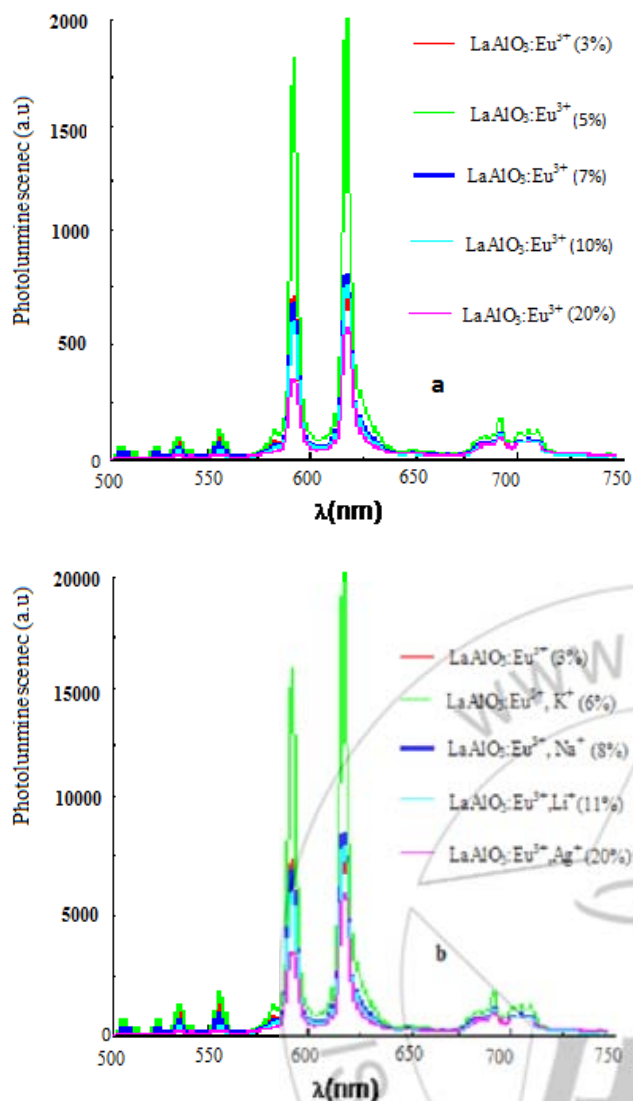


Figure 3: PL spectra of (a) $\text{LaAlO}_3:\text{Eu}^{3+}$ (b) $\text{LaAlO}_3:\text{Eu}^{3+}$ [Li^+ , Na^+ , K^+ , Ag^+] phosphors showing enhanced red emission

There is no significant effect on the structure of $\text{LaAlO}_3:\text{Eu}^{3+}$ co-doped with monovalent ions [Li^+ , Na^+ , K^+ , Ag^+] as the ionic radii of Eu^{3+} , Na^+ & Ag^+ correspond to 94.7 pm, 102 pm & 115 pm respectively are not much different from that of La^{3+} (103.7 pm), therefore these ions are likely to substitute for La^{3+} ion and act as the luminescence centers [23]. But Li^+ ions and K^+ ions have ionic radii 76 and 138 nm respectively having a large difference, are also incorporated in LaAlO_3 lattice successfully, due to this difference of ionic radii of Li^+ and K^+ ions, the LaAlO_3 lattice had slight deformations which lead to the variation in the heights of diffraction peaks in their patterns. As the ionic radius of Li^+ ion is less, there is a possibility of some of the ions to reside in interstitial sites between or among the host ions. For Na^+ ions [102pm], they could be located at La^{3+} [103.7pm] sites more easily than for K^+ ions [138pm] because of their bigger ionic radii than La^{3+} [103.7pm].

In fig.1, note that the XRD diffractogram of $\text{LaAlO}_3:\text{Eu}^{3+}$ nano - material co-doped with Li^+ , Na^+ , K^+ & Ag^+ ions were obviously almost identical but the relative intensities of crystal faces (111), (200) and (221) were different from each

other. We think this observation can be assigned to the enormous changes in lattice constants of these samples. The corresponding unit-cell constants and unit cell volumes of cubic $\text{LaAlO}_3:\text{Eu}^{3+}$ samples as well as doped with Li^+ , Na^+ , K^+ & Ag^+ are calculated from the distance between the adjacent (200) planes corresponding to diffraction peaks nearly $2\theta = 37.30^\circ \pm 4$ and are listed in Table 2.

Table2: The calculated lattice parameters of $\text{LaAlO}_3:\text{Eu}^{3+}$ co-doped with Li^+ , Na^+ , K^+ & Ag^+ ions

Phosphors	2θ	hkl/200	a (Å)	V (Å ³)
$\text{LaAlO}_3:\text{Eu}^{3+}$	37.341	2.406	4.8122	111.435
$\text{LaAlO}_3:\text{Eu}^{3+}, \text{Li}^+$	37.281	2.4098	4.8198	111.965
$\text{LaAlO}_3:\text{Eu}^{3+}, \text{Na}^+$	37.275	2.4101	4.8205	112.015
$\text{LaAlO}_3:\text{Eu}^{3+}, \text{Ag}^+$	37.27	2.4102	4.82	112.012
$\text{LaAlO}_3:\text{Eu}^{3+}, \text{K}^+$	37.257	2.4114	4.8228	112.175

It is noticed that if the ions with larger radius substitute the smaller cations in the crystalline lattice, the cell volume of the host compound is increased [25]. Therefore, as shown in Table 2, the cell volumes of $\text{LaAlO}_3:\text{Eu}^{3+}$ after co-doping with Na^+ , Ag^+ and K^+ ions increased, because the ionic radii of Na^+ ions (102 pm), Ag^+ (115pm) and K^+ ions (138 pm) are larger than that of La^{3+} ions (100 pm). The cell volume should decrease with the co-doping of Li^+ ions, but the cell volume of $\text{LaAlO}_3:\text{Eu}^{3+}$ co-doped with Li^+ ions increased, despite the fact that the Li^+ is smaller than La^{3+} . This increase may be due to the larger size of Li^+ ions than that of interstitial sites. We observed a remarkable improvement in the luminescence intensity of all emission peaks from Eu^{3+} particularly for $^5\text{D}_0 \rightarrow ^7\text{F}_2$ transition when the LaAlO_3 lattices is co-doped with monovalent ions [Li^+ , Na^+ , K^+ , Ag^+]. There is an increase of about 30, 50 and 500 % respectively in the luminescence intensity when monovalent ions [Li^+ , Na^+ , K^+ , Ag^+] are co-doped (fig.3 b). It seems that the co-doping of mono-valent ions increased the improved energy transfer from La^{3+} to Eu^{3+} and creating the oxygen vacancies which act as sensitizers [24] and facilitate the strong mixing of the La-O and Eu-O charge transfer states, and thus promote energy migration from the La-O CTS (charge transfer state) to Eu^{3+} . Further, more are the oxygen vacancies generated by co-doping of monovalent ions; more is the effective energy transfer between La^{2+} and Eu^{3+} ions. Finally, it can be concluded that the large increase in the emission intensity of the $^5\text{D}_0 \rightarrow ^7\text{F}_2$ transitions is due to improved energy transfer and reduced symmetrical environment around Eu^{3+} when co-doped with monovalent ions [Li^+ , Na^+ , K^+ , Ag^+] & co-doping had different effects on energy transfer ($\text{K}^+ > \text{Li}^+ > \text{Ag}^+ > \text{Na}^+$), which is in accordance with the sequence of luminescence from $^5\text{D}_0 \rightarrow ^7\text{F}_2$ transition of the Eu^{3+} .

In a similar case [25], the enhancement of Eu^{3+} luminescence intensity with the co-doping of alkali metals ions in Sr_2CeO_4 host lattice is due to the generation of oxygen vacancies to promote the energy transfer from Ce^{4+} to Eu^{3+} , reduce environment symmetry around Eu^{3+} ions and cause hole traps to quench the Ce-O CTS luminescence.

4. Conclusion

LaAlO₃:Eu³⁺ & LaAlO₃:Eu³⁺ [Li⁺, Na⁺, K⁺, Ag⁺] nano-phosphors are prepared by combustion synthesis method and the samples are further heated to 1000°C to improve the crystallinity of the materials. XRD analyses show that only trigonal phase is present in LaAlO₃:Eu³⁺ samples. Finally, it can be concluded that the large increase in the luminescence intensity of the ⁵D₀ → ⁷F₂ transitions is due to improved energy transfer and reduced symmetrical environment around Eu³⁺ when monovalent ions [Li⁺, Na⁺, K⁺, Ag⁺] are co-doped & co-doping had different effects on energy transfer (K⁺ > Li⁺ > Ag⁺ > Na⁺), which is in accordance with the sequence of luminescence from ⁵D₀ → ⁷F₂ transition of the Eu³⁺. The LaAlO₃:Eu³⁺ [K⁺] nano-material showing very high red luminescence of nearly 618 nm is definitely a material for further investigation for its use in red color display applications.

5. Acknowledgments

This nano-phosphor had been prepared in Inorganic Lab no 218, Deptt. of Chemistry, M.D.U Rohtak-124001, Haryana, India. by Dr. Subhash Chand Chopra, under supervision of Senior Professor Ishwar Singh, Pro-Vice Chancellor, P.D.M University, Bahadurgarh-124507, Haryana, India. & with support of Professor V.K. Sharma, H.O.D Chemistry, Department of Chemistry, M.D.U Rohtak.

References

- [1] O. V. Solov'yev, and B. Z. Malkin, "Modeling of electron-vibrational 4fⁿ–4fⁿ–15d spectra in LiYF₄:RE³⁺ crystals," *Journal of Molecular Structure*, 838, pp. 176-181, 2007.
- [2] K. Ogasawara, S. Watanabe, H. Toyoshima, M.G. Brik, "Handbook on Physics and Chemistry of Earths", 37, pp.1-59, 2007.
- [3] C. Shi, J. Shi, J. Deng, Z. Han, Y. Zhou, G. Zhang, *J. Electron Spectrosc. Phenom.*, **79**, 121, 1996
- [4] Z. Mao, D. Wang, Q. Lu, W. Yu, Z. Yuan, *Chem. Commun.*, **3**, 346-348, 2009
- [5] M. N. Popova, *J. Magn. Mater.*, **321**, 716, 2009.
- [6] Y. Bae, K. Lee, S. Byeon, *J. Lumin.*, **129**, 81, 2009.
- [7] L. Zhou, B. Yan, *J. Phys. Chem. Solids.*, **69**, 2877, 2008.
- [8] Y. Huang, C. Jiang, Y. Cao, L. Shi, H. Seo, *Mater. Res. Bull.*, **44**, 793, 2009.
- [9] T. Kijima, T. Shinburi, M. Sekita, G. Sakai, *J. Lumin.*, **128**, 311, 2008.
- [10] H. Kharbache, R. Mahiou, P. Boutinaud, D. Boyer, D. Zakaria, P. Deren, *Opt. Mater.*, **31**, 558, 2009.
- [11] P. Deren, J. Krupa, *J. Lumin.*, **102**, 386, 2003.
- [12] D. Hreniak, W. Strek, P. Dereń, A. Bednarkiewicz, A. Łukowiak, *J. Alloys Compd.*, **408**, 828, 2006.
- [13] D. Perez, A. Vegas, *Acta Cryst.*, **59**, 305, 2003.
- [14] L. Pieterse, M. Heeroma, E. Heer, A. Meijerink, *J. Lumin.*, **91**, 177, 2000.
- [15] F. Abbattista, M. Vallino, *Ceramics International.*, **9**, 35, 1938
- [16] S. Ekambaram, K. Patil, *J. Alloys Compd.*, **248**, 7, 1997.
- [17] R. Ningthoujam, V. Sudarsan, S. Kulshreshtha, *J. Lumin.*, **127**, 747, 2007.
- [18] X. Gao, L. Lei, C. Lv, Y. Sun, H. Zheng, Y. Cui., *J. Solid State Chem.*, **181**, p.1776, 2008.
- [19] G. Liu, G. Hong, J. Wang, X. Dong, *J. Alloys Compd.*, **432**, 200, 2007.
- [20] E. Perea, M. Estrada, M. Gracia, *J. Phys.*, **31**, 7, 1998.
- [21] T. Hayakawa, N. Kamt, K. Yamada, *J. Luminesc.*, **68**, 179, 1996.
- [22] G. Blasse, B. Grambler, *Luminescent Materials*, Springer-Verlag, 1994, p.43.
- [23] X. Xiao, B. J. Yan, *Mater Lett.*, 2007, **61**, 1649, 2007.
- [24] D. V. Voort, A. Imhof, G. Blasse, *J. Solid State Chem.*, **96**, 311, 1992.
- [25] Li-Li Shi, Yu Li Cheng, Su Qiang, *J. Fluorescence* **21**, 1461, 2011.

Author Profile



Dr. Subhash Chand, is a senior research scholar in the Department of Chemistry, M.D. University Rohtak-124001, Haryana, India and working on nanomaterial synthesis since 2008. Dr. Subhash Chand had published five research paper in International Journal indexed with Thomson Reuter. He presented four paper in national conference. One research paper is presented and published in international conference held at MIMT, Kota, Rajasthan, India. He attended two national workshop and also participated two times in state level science exhibition.